ISSN: 0369-8963

Entropy Analysis of Magneto-Nanofluid Flow in Vertical Channel with Variable Viscosity, In Coexistence with Activation Energy and Exothermic Chemical Reaction

Dr. Gnanaprasunamba K
Associate Professor, Department of Mathematics
Government First Grade College, Kurugodu, Ballari(Dist), Karnataka, India

Abstract : An attempt has been to investigate the impact of activation energy, variable viscosity, entropy generation on convective heat transfer flow of nanofluid in vertical channel with Brownian motion and thermo pharoses effects. The nonlinear governing equations have been solved by Runge-Kutta shooting technique. The velocity, Temperature and nanoconcentration, entropy generation have been analyzed to difference variations through graphs. The rate of heat and mass transfer has been evaluated numerically. It is found that an increase in viscosity parameter (B) enhances the velocity, temperature and reduces the nanoconcentratioin. The skin friction grows Sherwood number enhances and Nusselt number decays at the left wall and opposite effect is seen in them at the right wall. Increase in reaction rate parameter(Q1) results in growth of the momentum boundary layer thickness.
Keywords : Heat and Mass transfer, Variable Viscosity, Activation Energy, Brownian motion, Entropy generation, exothermic chemical reaction.

1. INTRODUCTION :

There are a number of possible uses for the interaction of magnetic fields with nanofluids, including the cooling of nuclear reactors using liquid sodium and the induction of a flow metre that relies on the fluid's potential difference along a direction perpendicular to both the magnetic field and motion. The inability of chemotherapy to provide localised drug targeting increases the harmful effects on nearby tissues and organs. The magnetic drug targeting does this exactly. The foundation of this technique is the binding of well-known anticancer medications with magnetic nanoparticles, which can use a magnetic field to concentrate the medication in the tumour location. Because of its numerous applications in various technical and industrial domains, MHD has attracted the attention of scientists and researchers. Various scientists and researchers have applied the MHD in various fields of study based on these applications. The effect of the chemical reaction on the three-dimensional flow of Maxwell nanofluid across a stretched surface with a magnetic field was investigated by Das et al. [6], Reddy and Lakshminarayana [21].

Energy is known to decay as it changes forms, and the pace at which it does so in a thermal process is quite concerning. This has been a significant obstacle in the processes of energy conversion and management. The combined effects of temperature and velocity gradients are what cause the entropy formation. Wang et al. [25], for example, discussed the entropy optimised flow across a nonlinear stretched surface where nanomaterial was present. In order to study the thermodynamic analysis for a stagnation point and a porous expanding sheet with a heat source, Rashidi et al. [20] used a semi-analytical technique. The investigation of entropy generation in a transient radiated flow of magnetohydrodynamic viscous fluid was described by

 https://doi.org/10.5281/zenodo.14868720

Muhammad and Khan [17] and Nayak et al. [18]. In the recent study of Abbas et al. [1,2], a numerical examination of entropy optimized Darcy-Forchheimer flow with MHD on Molybdenum disulfide (MOS2) and Silicon dioxide (SiO2) hybrid nanofluid over a stretched surface is considered. Many more researchers (Khan et al. [13], Afridi and Qasim [4], and Mondal [16], Adesanya et al. [3], Riaz Muhammad et al.[22] and Yusuf et.al.[27], Essma Belahmadi and Rachid Bessaih [7] are also employed the heat transfer and entropy generation analysis of Cu-water nanofluid in a vertical channel. Zaheer Abbas et al[28], Kahalerras et al [12], Hammed Abiodun Ogunseye and Precious Sibanda [10] have been discussed the analysis of entropy generation for MHD flow of viscous fluid embedded in a vertical porous channel with thermal radiation, porous channel with copper-water nanofluids. Nidhish et al [19] have analyzed the electroosmotic MHD ternary hybrid Jeffery nanofluid flow through a ciliated vertical channel with gyrotactic microorganisms: Entropy generation optimization. Also Michael Hamza Mkwizu and Oluwole Daniel Makinde [15] have extended the entropy generation in a variable viscosity channel flow of nano fluids with convective cooling.

A key idea in chemical kinetics, activation energy is frequently covered in physical chemistry classes. Svante Arrhenius, a Swedish physicist, coined the phrase "activation energy" in 1889. Current advances in the calculation and interpretation of the activation energy of a kinetic technique are described. Currently, the fluctuation theory of statistical mechanics applied to kinetics is used to directly estimate the energy needed to activate for an infinite cyclical timescale from simulations at a single temperature. This gives active processes more choices when a standard Arrhenius analysis is impractical. The techniques enable the methodical breakdown of activation energy into elements linked to the many interactions and motions of the system. Several authors have been evaluated to effect of Arrhenius activation energy and dual stratifications on the MHD flow of a Maxwell nanofluid with various heating (Gayathri[8], Gireesha et al. [9], Sandhya et al. [24], Zeeshan et al. [29], Saida Rashid et al. [23]). Khan et al [14], Ijaj Khan et al [11], made brief discussion on Activation Energy impact in Nonlinear Radiative Stagnation Point Flow of Cross Nanofluid and also analysed the Arrhenius activation energy impact in binary chemically reactive flow of TiO_2-Cu-H_2O hybrid nanomaterial.

The goal of research on thermal stability and heat transmission in flammable materials exposed to oxidation chemical reactions is to guarantee the security of their use, storage, and transportation. Reactive hazard evaluation includes this crucial practical component (Lohrer et al., [36]; Tanaka et al., [39]; Bowes, [35]). Numerous research have been carried out to evaluate the induction time of an explosion, assuming it occurs, and to identify the essential parameters that divide the explosive and non-explosive domains of a subsequent reaction (Simmie [38]; Balakrishnan et al., [34]; Makinde [37]). Specifically, they make it possible to estimate runaway characteristics early in a chemical product's life cycle, which guarantees the abolition or substantial reduction of the need for explosive tests (Williams [40]). The two branches of theoretical approach—the family of semi-analytical approaches and more complex numerical simulation methods—are also united by the method based on the mathematical theory of combustion. Legodi and Makinde [42] investigated a steady state exothermic process in a slab with convective boundary conditions using numerical methods. Using a spectral collocation approach, Obalalu et al. [31, 32, 33] and Adeshina et al. [30] have examined how the variable electrical conductivity affects the thermal stability of the MHD reactive squeezed fluid flow through a channel when Arrhenius energy and an exothermic chemical reaction coexist.

 https://doi.org/10.5281/zenodo.14868720

ISSN: 0369-8963

This paper an attempt has been to investigate the impact of activation energy, variable viscosity, entropy generation on convective heat transfer flow of nanofluid in vertical channel with Brownian motion and thermo pharoses effects. The nonlinear governing equations have been solved by Runge-Kutta shooting technique. The velocity, Temperature and nanoconcentration, entropy generation have been analyzed to difference variations through graphs. The rate of heat and mass transfer has been evaluated numerically.

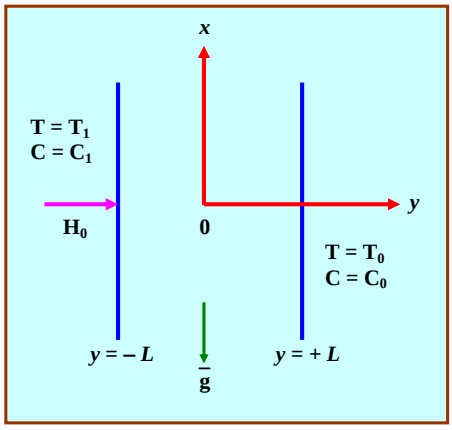

Fig.1. Schematic diagram of the problem under consideration

2.FORMULATION OF THE PROBLEM:

Consider the steady flow of an electrically conducting, viscous fluid through a porous medium in a vertical channel by flat walls. A uniform magnetic field of strength Ho is applied normal to the walls. Assuming the magnetic Reynolds number to be small we neglect the induced magnetic field in comparison to the applied field. The walls are maintained at constant temperature T_1 ,T_0 and concentration C_1,C_0 respectively. We consider a rectangular Cartesian coordinate system O(x,y) with x-axis along the walls and y-axis normal to the walls. The walls are taken at $y = \pm 1$. The boundary layer equations of flow ,heat and mass transfer under Boussinesq approximation, and following Buongiorno model (2006) are:

Equation of Continuity

$$\frac{\partial u}{\partial x} = 0 \tag{1}$$

Momentum equation

$$0 = -\frac{\partial p}{\partial x} + \frac{\partial}{\partial y}(\mu_f(T)\frac{\partial u}{\partial y}) - \frac{\sigma B_o^2}{\rho_f}u - \frac{\mu_f(T)}{k_p}u + g(1-C_0)\beta\rho_{f_\infty}\beta g(T-T_0) - \\ -(\rho_p - \rho_{f_0})g(C-C_0) \tag{2}$$

Energy equation

$$0 = \alpha_f\frac{\partial^2 T}{\partial y^2} - \frac{1}{\rho C_p}\frac{\partial(q_R)}{\partial y} + \tau(D_B\frac{\partial T}{\partial y}\frac{\partial C}{\partial y} + (\frac{D_T}{T_m})(\frac{\partial T}{\partial y})^2) + \\ + \frac{\alpha_f\mu_f(T)}{\rho C_p}(\frac{\partial u}{\partial y})^2 + \frac{\sigma B_o^2}{\rho C_p}(u^2) + \frac{QA}{k_T}(\frac{T}{T_o})^n(C-C_0)Exp(-\frac{E_n}{KT}) \tag{3}$$

https://doi.org/10.5281/zenodo.14868720

ISSN: 0369-8963

Diffusion equation

$$0 = D_B \frac{\partial^2 C}{\partial y^2} + (\frac{D_T}{T_m}) \frac{\partial^2 T}{\partial y^2} - k_c (C - C_o)(\frac{T}{T_0})^n Exp(-\frac{E_n}{kT}) \quad (4)$$

The boundary conditions relevant to the problem are

$$\begin{aligned} u(-1) = 0, T = T_1, C = C_1 \quad on\ y = -L \\ u(+1) = 0, T = T_o, C = C_o \quad on\ y = +L \end{aligned} \quad (5)$$

Where u is the velocity, T, C are the fluid temperature and concentration. T1, To, C1, Co ate temperature and concentration on the left and right walls(±L). σ, μe are the electrical conductivity, magnetic permeability.μf is the variable viscosity of the fluid,ρ is the fluid density, p is the fluid pressure, kp coefficient of porous medium, D_B,D_T are the mass diffusivity coefficient, chemical molecular diffusivity, kc is the chemical reaction coefficient, Q is heat of reaction, A is rate constant, K_T is Boltzmann constant En is Arrhenius coefficient of activation energy, R is the Stefan –Boltzmann constant and q_R is the radiative heat flux.

By using Rosseland approximation for radiative heat flux, qr is simplified as

$$q_r = -\frac{4\sigma^{\bullet}}{3\beta_R} \frac{\partial T'^4}{\partial y} \quad (6)$$

where $\sigma^{\bullet}$=5.6607x10^{-8} Wm^{-2}K^{-4} is the Stefan –Boltzman constant and β_R is the Rosseland mean absorption coefficient. In the case of nanofluid, herein (optically thick) the thermal radiation travels only a short distance before being scattered or absorbed. If the temperature differences within the fluid flow are sufficiently small, T'^4 may be expressed as a linear combination of temperature. This is done by expanding T'^4 in a Taylor series about top wall temperature Ti as follows:

$$T'^4 \ ; \ T_o^4 + 3T_o^3(T - T_o) + 6T_o^2(T - T_o)^2 + ---- \quad (7)$$

Neglecting higher order terms in the above equation beyond the first order in $(T - T_o)$,we get

$$T'^4 \cong 4T_o^3 T - 3T_o^4 \quad (8)$$

In view of the equations(6&8),equation(3) becomes

$$0 = (\alpha_f + \frac{16\sigma^{\bullet} T_o^2}{3\beta_R}) \frac{\partial^2 T}{\partial y^2} \frac{1}{\rho C_p} \frac{\partial (q_R)}{\partial y} + \tau (D_B \frac{\partial T}{\partial y} \frac{\partial C}{\partial y} + (\frac{D_T}{T_m})(\frac{\partial T}{\partial y})^2) +$$

$$+ \frac{\alpha_f \mu_f (T)}{\rho C_p} (\frac{\partial u}{\partial y})^2 + \frac{\sigma B_o^2}{\rho C_p} (u^2) - \frac{QA}{k_T} (\frac{T}{T_o})^n (C - C_0) Exp(-\frac{E_n}{KT})$$

The dynamic viscosity of the nanofluids is assumed to be temperature dependent as follows:

$$\mu_f (T) - \mu_o Exp(-m(T - T_o)) \quad (9)$$

where μ_o is the nanofluid viscosity at the ambient temperature To. m is the viscosity variation parameter which depends on the particular fluid.

Introducing non-dimensional variables as

$$\eta = \frac{y}{L}, u' = \frac{uL}{\mu_o}, \theta = \frac{T - T_o}{T_1 - T_o}, \varphi = \frac{C - C_o}{C_1 - C_o}, p' = \frac{pL^2}{\mu_o^2} \quad (10)$$

The equations (2-4) reduce to

 https://doi.org/10.5281/zenodo.14868720

ISSN: 0369-8963

$$\frac{d^2u}{dy^2} - B\frac{du}{dy}\frac{d\theta}{dy} - Ku + e^{b\theta}(A - M^2u + Gr(\theta - N\phi)) - fs(\frac{du}{dy})^2 = 0 \quad (11)$$

$$(1+\frac{4Rd}{3})\frac{d^2\theta}{dy^2} + Nb\frac{d\theta}{dy}\frac{d\varphi}{dy} + Nt(\frac{d\theta}{dy})^2 + Ec(e^{-B\theta})(\frac{d^2u}{dy^2})^2 + \\ +EcM^2(\frac{du}{dy})^2 + \lambda(1+n\delta\theta)e^{-\frac{E_1}{(1+\delta\theta)}} = 0 \quad (12)$$

$$\frac{d^2\phi}{dy^2} + (\frac{Nt}{Nb})\frac{d^2\theta}{dy^2} - \gamma\, Sc(1+n\delta\theta)Exp(-\frac{E_1}{1+\delta\theta}) = 0 \quad (13)$$

The corresponding boundary conditions are

$$u(-1) = 0, \theta(-1) = 1, \varphi(-1) = 1 \\ u(+1) = 0, \theta'(+1) = 0, \varphi(+1) = 0 \quad (14)$$

Where

$$Gr = \frac{\beta_T g(T_1 - T_0)L^3}{\mu_o^2}, M = \frac{\sigma B_o^2 L^2}{\mu_o}, K = \frac{L^2}{k_p}, N = \frac{\beta_C(C_1 - C_0)}{\beta_T(T_1 - T_0)}, B = m(T_1 - T_0),$$

$$Nb = \frac{\tau D_B(C_1 - C_0)}{\alpha_f}, Nt = \frac{\tau D_T(T_1 - T_0)}{\alpha_f}, \theta_w = \frac{T_1}{T_o}, \delta = \theta_w - 1,$$

$$E_1 = \frac{E_n}{k_f T_0}, Ec = \frac{\mu_0}{k_f L^2(T_1 - T_0)}.Sc = \frac{\nu}{D_B}, \mathrm{Q}_1 = \frac{QAL^2(C_1 - C_0)}{k_T}$$

are the Grashof number, magnetic parameter, Darcy parameter, buoyancy ratio, viscous parameter, Brownian motion parameter, thermophoresis parameter, temperature difference parameter, activation energy parameter, Eckert number, Schmidt parameter, Frank-Kameneskii constant(reaction rate parameter).

3.NUMERICAL ANALYSIS:

The coupled non-linear ODEs (11)-(13) along with the corresponding Bcs(14) are solved by employing the RKF algorithm with Mathematica programming. The numerical solutions are carried out by choosing the step size Δη=0.001.

(i)The coupled non-linear system of equations was transformed into a set of first order Des.

$$f = f_1, f' = f_2, f'' = f_3, \theta = f_4, \theta' = f_5, \phi = f_6, \phi' = f_7$$

(ii)The system of first order Des are

$$f''' = (Bf_2 f_4 + Kf_1) - e^{Bf_4}(A - M^2 f_1 + Gr(f_4 - Nf_6))$$

$$\theta'' = -(Nbf_5 f_7 + Ntf_5^2 + Ece^{-Bf_4} f_3^2 + Q_1 f_6 (1 + n\delta f_4)e^{-E1/(1+\delta f_4)}$$

$$\varphi'' = -(\frac{Nt}{Nb})(f_4 f_6 + Nt^2 f_4^2 + Ece^{-Bf_4} f_3^2 + EcM^2 f_2^2) + \gamma Sc)(1 + n\delta f_4)e^{-E1/(1+\delta f_4)})$$

The boundary conditions are

$$f_1(\pm 1) = 0, f_4(-1) = 1, f_4(+1) = 0, f_6(-1) = 1, f_6(+1) = 0$$

https://doi.org/10.5281/zenodo.14868720

ISSN: 0369-8963

(iii) Suitable guess values are chosen for unknown required Bcs.
(iv) RKF technique with shooting method is utilized for step by step integration with the assistance of Mathematica software.

4.SKIN FRICTION.NUSSELT AND SHERWOOD NUMBER:

The quantities of physical interest in this analysis are the skin friction, coefficient Cf, local Nusselt number(Nu),local Sherwood number(Sh) which are defined as

$$C_f = \frac{2\tau_w}{\rho u_w^2}, Nu = \frac{xq_w}{\alpha_f (T_1 - T_o)}, Sh = \frac{xm_w}{D_B (C_1 - C_o)} \tag{4.1}$$

where $\tau_w = \mu(\frac{\partial u}{\partial y})_{\eta=\pm1}, q_w = k_{nf}(\frac{\partial T}{\partial y})_{\eta=\pm1}, m_w = D_B(\frac{\partial C}{\partial y})_{\eta=\pm1}$ (4.2)

Substituting equation(4.2) into equation (4.1),we get

$$Cf = e^{-B\theta}\frac{\partial u}{\partial \eta})_{\eta=\pm1}, Nu = -(\frac{\partial \theta}{\partial \eta})_{\eta=\pm1}, Sh = -(\frac{\partial \Phi}{\partial \eta})_{\eta=\pm1} \tag{4.3}$$

5.ENTROPY GENERATION:

In nanofluid flows, the improvement of the heat transfer properties cause a reduction in entropy generation (Ns). However a convection process involving a channel flow of nanofluids is inherently irreversible. The non-equilibrium due to exchange of energy and momentum within the nanofluid and at solid surface ,cause continuous entropy generation .one part of this entropy production results from heat transfer in the direction of the finite temperature gradients, while another part arises due to the fluid friction, nanoparticle concentration and complex interaction between the base fluid and the nanoparticles. According to Wood's (1975) the local volumetric rate of entropy generation is given by

$$S''' = \frac{k_f}{T_o^2}(\frac{knf}{k_f} + \frac{16\sigma^* T_o^2}{3\beta_R})(\frac{\partial T}{\partial z})^2) + \frac{\mu_{nf(T)}}{T_0^2}(\frac{\partial u}{\partial z})^2 + \frac{\sigma_{nf} B_o^2}{T_0}(u^2) + \frac{D_B}{C_0}(\frac{\partial C}{\partial z})^2 + \frac{D_B}{T_0}(\frac{\partial T}{\partial z}\frac{\partial C}{\partial z})$$

where the first term in t he irreversibility due to the heat transfer, the second is the entropy generation due to the viscous dissipation , the third term is the local entropy generation due to the effect of the magnetic field (Joule heating or Ohmic heat)and the last term is local entropy generation due to mass transfer of the nanoparticles and their complex interact ion with the base fluid.

In non-dimensional form

$$N_s = \frac{a^2 S'''}{k_f} = (\frac{4Rd}{3} + A_5)(\frac{\partial \theta}{\partial \eta})^2 + \frac{Br}{\Omega}[e^{-B\theta}((\frac{\partial u}{\partial \eta})^2 + M^2 A_6 (u)^2] + \lambda[(\frac{\partial \varphi}{\partial \eta})^2 + (\frac{\partial \varphi}{\partial \eta})(\frac{\partial \theta}{\partial \eta})]$$

where $\mathrm{Br} = \mathrm{EcPr}(\text{Brinkmann number}), \Omega = \frac{T_1 - T_0}{T_o}$ (*Temperature difference*)

$$\lambda = \frac{C_o D_B}{k_f} (\textit{nanoparticles mass transafer parameter})$$

https://doi.org/10.5281/zenodo.14868720

ISSN: 0369-8963

$$Let\ N_1 = \frac{k_{nf}}{k_f}(1+\frac{4Rd}{3})(\frac{\partial\theta}{\partial\eta})^2, N_2 = \frac{Br}{\Omega}[e^{-B\theta}((\frac{\partial u}{\partial\eta})^2 + \mathrm{M}^2(\mathrm{u}^2)], N_3 = \lambda[(\frac{\partial\Phi}{\partial\eta})^2 + \frac{\partial\Phi}{\partial\eta}\frac{\partial\theta}{\partial\eta}]$$

$$\text{Irreversability ratio is defined by } \phi = \frac{N_2}{N_1 + N_3}$$

Heat and nanoparticles mass transfer irreversibility dominates for $0 \le \phi < 1$ and fluid friction irreversibility dominates when $\phi>1$. The contributions of both irreversibility's to entropy generation are equal when $\phi=1$.We define the Bejan number (Be) mathematically as Be=(N1+N3)/N2=1/(1+ϕ1). This shows that Be ranges from 0 to 1. Be=0 implies that the limit where irreversibility is dominated by the effect of fluid friction, while Be=1 is the limit where the irreversibility due to heat and nanoparticles mass transfer dominates the flow systems. Heat and Mass transfers together with fluid friction irreversibility are the same when Be=0.5.

6. COMPARISON :

In the absence of exhothermic chemical reaction (Q1=0) the results are good agreement with Nagasasikala [42]

Parameter		Nagasasikala [42]				**Present Results**			
		η= – 1		η = +1		**η= – 1**		**η = +1**	
		Nu(–1)	Sh(–1)	Nu(–1)	Sh(–1)	**Nu(+1)**	**Sh(+1)**	**Nu(+1)**	**Sh(+1)**
B	0.25	0.07453	0.98147	0.93152	0.04905	**0.07450**	**0.98148**	**0.93156**	**0.04917**
	0.5	0.04807	1.00699	0.95859	0.02291	**0.04860**	**1.00696**	**0.95862**	**0.02295**
	0.75	0.02293	1.03127	0.98384	-0.01145	**0.02289**	**1.03122**	**0.98389**	**-0.01146**
Nb	0.2	0.03797	0.82297	0.03797	0.82297	**0.03792**	**0.82298**	**0.03799**	**0.82298**
	0.3	0.02886	0.76527	0.01864	0.76527	**0.02885**	**0.76529**	**0.01865**	**0.76529**
Nt	0.3	0.01463	1.56261	0.01759	1.56261	**0.01465**	**1.56265**	**0.01762**	**1.56265**
	0.5	0.00973	1.97404	0.01274	1.97404	**0.00977**	**1.97406**	**0.01282**	**1.97406**
E1	0.3	0.07462	0.97205	0.93192	0.05187	**0.07465**	**0.97207**	**0.93195**	**0.05189**
	0.5	0.07475	0.96483	0.93225	0.05404	**0.07470**	**0.96489**	**0.93228**	**0.05406**
Pr	1.71	0.24663	0.90836	0.73074	0.21045	**0.24665**	**0.90838**	**0.73075**	**0.21046**
	6.20	0.24641	0.92708	0.73041	0.20558	**0.24645**	**0.92710**	**0.73045**	**0.20559**

* B=0.25, Nb=0.1,Nt=0.2,E1=0.1,Pr=0.71 are common values.

7. RESULTS and DISCUSSION:

In this analysis we investigate the effect of variable viscosity and Arrhenius activation energy on convective heat and mass transfer flow of nanofluid in a vertical channel bounded by flat walls which are maintained at uniform temperature and concentration on the walls in the presence of heat sources.

Figs.2a-2c exhibit the effect of Grashof number(G) and magnetic parameter(M) on the velocity, temperature and concentration From the profiles we find that the velocity, temperature experience a depreciation while the concentration increases in the flow region with increasing values of G. This shows that an increase in G decays the thickness of the momentum, thermal boundary layers and grows solutal layer thickness.Fig.2a exhibits the decreasing nature of the velocity profiles for growing strength of magnetic force. Physically, a retarding force or drag

 https://doi.org/10.5281/zenodo.14868720

ISSN: 0369-8963

force (Lorentz force) is generated due to the presence of a magnetic force. On the other hand the heat measure enhances and the mass of the fluid are depicted in figures 2b&c. Hence, by controlling the magnetic force, the required cooling can be achieved, which is useful in many engineering applications. For higher values of M we notice an enhancement in temperature and deceleration in concentration in the flow region. Thus higher the magnetic parameter smaller the thickness of the momentum and solutal boundary layer, larger the thermal boundary layer thickness.

The effect of porous medium (K) and viscosity variation(B) on flow variables can be seen from figs.3a-3c.From the profiles we noticed that lesser the permeability of the porous medium smaller the velocity ,concentration and larger the tempe3rature in the flow region. From the profiles we find that the effect of viscosity variation(B) lead to a to a rise in velocity and decay in concentration. The temperature reduces with viscosity parameter(B) in the flow region((figs.3a-3c).This implies that variation in viscosity leads to a growth in momentum boundary layer thickness and decay in thermal, solutal layers.

Figs.4a-4c represent the effect of Brownian motion(Nb) and thermophoresis parameter (Nt) on flow variables. An increase in Nb leads to a depreciation in velocity, rise in temperature and nanoparticle concentration while velocity reduces, temperature and nanoparticle concentration grows with rise in thermophoresis parameter(Nt). Physically, thermophoretic force creates a retardation flow in the flow region. Consequently, as Nt increases the thickness of the thermal and solutal boundary layers decay(figs.4a-4c).

Figs.5a-5c represent the effect of thermal radiation(Rd) and Eckert number(Ec) on the flow variables. From the profiles we find that higher the thermal radiative heat flux, smaller the velocity and thermal temperature while the nanoconcentration experiences enhancement bin the flow region. This may be attributed to the fact that the thickness of the momentum, thermal boundary layers become thinner, solutal layer becomes thicker with increase in Rd. Higher the dissipative energy(Ec) smaller the velocity and larger the temperature the actual nanoparticle concentration. This implies an increase in Ec leads to a decay in momentum and growth in thermal and solutal boundary layers.

The effect of chemical reaction on flow variables can be seen from figs.6a-6c.The velocity increases, temperature and, actual nanopaticle concentration depreciates in the degenerating chemical reaction case. This may be attributed to the fact that an increase in $\gamma>0$ leads to growth of momentum layer, thermal and solual boundary layers .In generating chemical reaction case, velocity experiences enhancement, temperature and nanoparticle concentration depreciate in the flow region.

Figs.7a-7c exhibit the effect of temperature relative parameter(δ) and activation energy parameter(E1) on flow variables. From the profiles we find that the temperature and nanoparticle concentration dilute ,velocity upsurges with rising values of δ .An increase in activation energy parameter(E1) leads to a decay in momentum layer, growth in thermal and solutal layer thickness in the flow region. This is due to the fact that an increase in temperature relative parameter(δ) leads to thinning of the thickness of the thermal and solutal boundary layers while they become thicker in the flow region with E1.

Figs.8a-8c exhibit the effect of Schmidt number(Sc) and reaction rate parameter(Q1) on flow variables. It is observed from the profiles that the velocity, nanoparticle concentration increase and temperature decreases with a rise in Sc. In fact, Schmidt expresses the relative contribution of thermal diffusion rate to species diffusion rate in the flow region. A large Schmidt number has a relatively lower molecular diffusivity. Therefore, a gradual increase in Sc

 https://doi.org/10.5281/zenodo.14868720

ISSN: 0369-8963

corresponds to a thicker concentration boundary layer, as in evident from fig.8c.With respect to reaction rate parameter(Frank-Kameneskii constant)

We notice a reduction in velocity, temperature and nanoparticle concentration with a rise in Prandtl number. Physically, thermal diffusivity decreases with increasing values of Pr. This indicates that thickness of momentum, thermal and solutal boundary layers become thinner in the flow region with rise in Pr.

The effects of governing parameters on entropy generation(Ns) are presented in figs.2d-11d. The effect of Grashof number(G) and magnetic parameter(M) on the entropy generation number (Ns) is shown in fig.2d.The entropy generation number decreases with increase in G and increases with rising values of magnetic parameter(M) in the vicinity of the left wall(η=-1) while changes are insignificant while moving towards the right wall(η=+1).An increase in the magnetic field intensity causes the resistance of the force against the fluid movement, resulting in the increase of the heat transfer rate in the boundary layer. It reveals that the magnetic field is a source of the entropy generation in addition to the fluid friction and heat transfer. Also it is observed that the entropy generation is prominent at the surface of the left wall of the channel and in the region close to the wall η=-1.This implies that ,in order to control the entropy generation which is generated in the boundary of the flow, the magnetic parameter must be reduced, which is an interest topic in the nuclear –MHD propulsion.Fig.3d illustrate Ns with inverse Darcy parameter(K) and Viscosity parameter(B).An increase in K increase the entropy generation while higher the viscosity parameter(B) smaller the entropy generation(Ns) in the region adjacent to left wall(η=-1).Fig.4d represents Ns with Brownian motion parameter(Nb) and Thermophoresis parameter(Nt).Increase in Nb enhances the entropy generation(Ns) and reduces with Nt .The is due to the fact that the entropy generation due to heat transfer, viscous dissipation and mass transfer of the nanoparticle interaction w3ith the base fluid increases with Nb and decays with Nt in the boundary layer flow.Fig.5d exhibit Ns with radiation parameter (Rd) and Eckert number(Ec).From the profiles it is found that the entropy generation(Ns) increases with higher values of Rd and decays with increases dissipative energy in the flow region. Fig.6d shows that the entropy generation(Ns) experiences reduction in the degenerating chemical reaction and upsurges in generating chemical reaction case. The effect of activation energy parameter (E1) and temperature difference ratio(δ) on entropy generation can be seen from fig.7d. Higher the activation energy results in an enhancement in entropy generation(Ns) and decay with larger values of temperature difference ratio(δ).From fig.8d it is noticed that lesser the molecular diffusivity/reaction rare parameter(Q1)smaller the entropy generation in the entire flow region. Fig.9 demonstrates the variation of entropy generation with nanoparticle mass transfer parameter(λ) and group parameter($\mathrm{Br}\,\Omega^{-1}$). From the profiles it is noticed that the entropy generation(Ns) reduces with increase in both λ and Br Ω^{-1}. This is because higher Br Ω^{-1} and nanoparticle mass transfer parameter(λ) decrease the nanofluid friction and entropy generation due to mass transfer of the nanoparticles and their interaction with the base fluid.

Effect of parameters on Bejan number(Be):

In order to study the heat transfer entropy generation dominates over the fluid friction, magnetic field and nanoparticle mass transfer entropy generation 0f vive versa, the Bejan number is lotte for different physical parameters in fdigs.2e-9e. Fig.2e shows that Bejan number(Be) enhances with rising values of Grashof number(G) and depreciates with magnetic parameter(M). For larger values of G ,the entropy generation due to viscous dissipation dominates over the combined entropy generation due to heat transfer and nanoparticle mass transfer, which results in an enhancement in Be in the fluid flow. For larger values of M, the entropy generation due to

 https://doi.org/10.5281/zenodo.14868720

the combined entropy generation due to heat transfer and nanoparticle mass transfer dominates over the entropy generation due to viscous dissipation. Fig.3e illustrates variation of Be with K and B.It is found that for larger values of inverse-Darcy parameter(K)/thermophoresis parameter (Nt)/ radiation parameter(Rd)/temperature difference ratio(δ)/reaction rate parameter (Q1) (figs.3e,4e,5e,8e),the combined entropy generation due to heat transfer and nanoparticle mass fraction dominates over the entropy generation due to viscous dissipation while opposite effect is noticed in Be with larger values of B/Nb/Ec/γ/E1/Sc/Q1(figs.3e,4e,5e,7e,8e). Fig.9e demonstrate the variation of Bejan number(Be) with group parameter($\mathrm{Br}\,\Omega^{-1}$) and nanoparticle volume fraction(λ). The Bejan number decreases with an increase in $\mathrm{Br}\,\Omega^{-1}$. This is quite true that because higher $\mathrm{Br}\,\Omega^{-1}$ can increase the magnitude of the irreversibility ratio (Φ) which in turn reduces the Bejan number(Be). Also increase in nanopartcle mass transfer parameter(λ) ,entropy generation due to combined influence of nanoparticle mass transfer and heat transfer (N1+N3) dominates over the entropy generation due to viscous dissipation (N2). The group parameter ($\mathrm{Br}\,\Omega^{-1}$) is important for the irreversibility analysis. It measures the relative importance of the viscous effects to that of temperature gradient entropy generation. The Bejan number profiles are useful for that whether the heat transfer irreversibility dominates the fluid friction irreversibility or not.

The skin friction factor(Cf),Nusselt (Nu)and Sherwood number (Sh)at the walls $\eta = \pm 1$ are exhibited in table.2.From the tabular values we observe that Cf, Nu and Sh decay with G, Cf decay with increasing values of M , K and enhance with M and K at η=-1 while at η=+1,Cf,Nu reduces with G,M enhances with K. Nu and Sh increase with G and K and reduces with higher values of M. When the molecular buoyancy force dominates over the thermal buoyancy force Cf, Sh reduces, Nu enhances at η=-1&at η=+1,Cf,Nu and Sh increase with N. Cf,Nu decay, Sh grows at η=-1 and at η=+1,Cf,Nu,Sh enhance with higher values of viscosity parameter(B). Higher the strength of the heat generating source(Q>)larger Cf, Nu, Sh while Cf, Sh reduce, Nu enhances with absorbing source(Q<0) at η=-1 and at η=+1,Cf reduces, Nu, Sh enhance with Q>0 and for Q<0,Cf,Sh increase, Nu reduces at the wall. Cf, Sh grow, Nu decay in degenerating chemical reaction case, while in generating case, Cf, Sh reduce, Nu enhances at η=-1.At η=1,Cf decays, Nu, Sh grows with γ>0 and in the case of γ<0,Cf,Sh grow, Nu decays at the wall.

An increase in Brownian motion parameter(Nb) reduces Cf,Sh and enhances Nu at the left wall and at the right wall, Cf increases, Nu and Sh. Cf, Sh enhance, Nu decay at η=-1 and at η=1,Cf reduces, Nu, Sh enhance with increase in thermophoresis parameter (Nt), Lewis number(Le),index (n).Higher the dissipation/Prandtl number, smaller Cf, Nu and Sh on the walls. Cf reduces at η=-1 and enhances at η=1 with increase in Ec/Pr. Cf grow with temperature relative parameter(δ) and decay with increasing values of activation energy parameter(E1),while Sh increases with δ and decreases with E1 on both the walls. The rate of heat transfer (Nu) reduces with δ and enhances with E1 at η=-1 while a reversed effect is noticed at η=1.In addition, AE(E1) plays an important role in increasing the local heat transfer coefficient. Generally, AE is the minimum amount of energy that is required for a chemical reaction to stimulates atoms or molecules in the reaction. There should a considerable number of atoms whose AE is less than or equal to translational energy in a chemical reaction, hence in many engineering applications, AE may be considered as a better coolant.

Effect of parameters on Entropy generation(Ns):

 https://doi.org/10.5281/zenodo.14868720

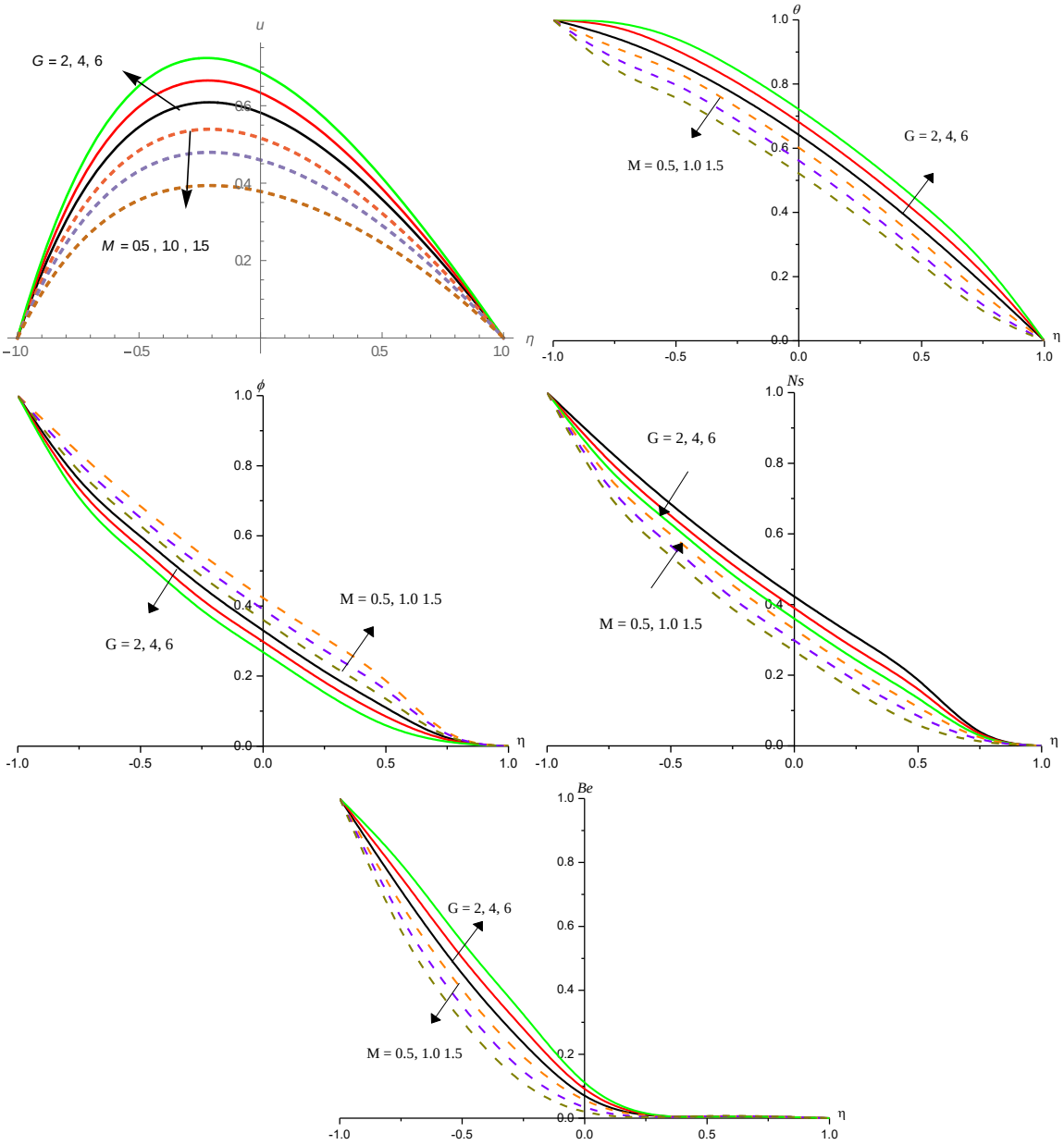

Fig.2 : Variation of [a] Velocity(u), [b] Temperature (θ), [c] Concentration (ϕ), [d] Entropy generation(Ns),
[e] Bejan number (Be) with G & M
B=0.25, K=0.2, Nb=0.1, Nt=0.2, Rd=0.5, Ec=0.05, γ=±0.5, E1=0.1, δ=0.2, Sc=0.24,Q1=0.5, Br=0.25, λ=0.5

https://doi.org/10.5281/zenodo.14868720

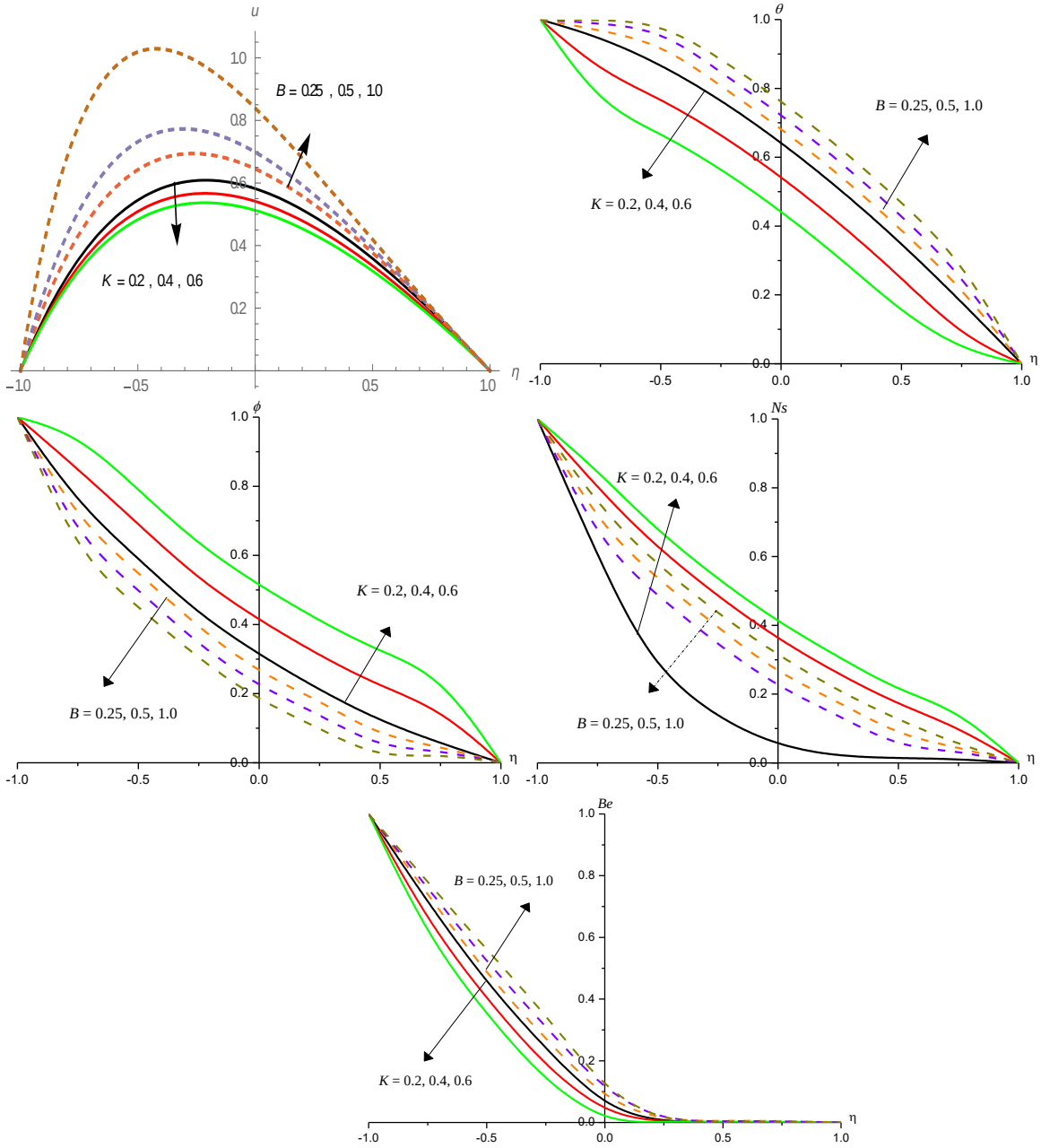

Fig.3 : Variation of [a] Velocity(u), [b] Temperature (θ), [c] Concentration (ϕ), Entropy generation(Ns) , [e] Bejan number (Be) with K & B
G=2, M=0.5, Nb=0.1, Nt=0.2, Rd=0.5, Ec=0.05, γ=±0.5, E1=0.1, δ=0.2, Sc=0.24,Q1=0.5, Br=0.25, λ=0.5

https://doi.org/10.5281/zenodo.14868720

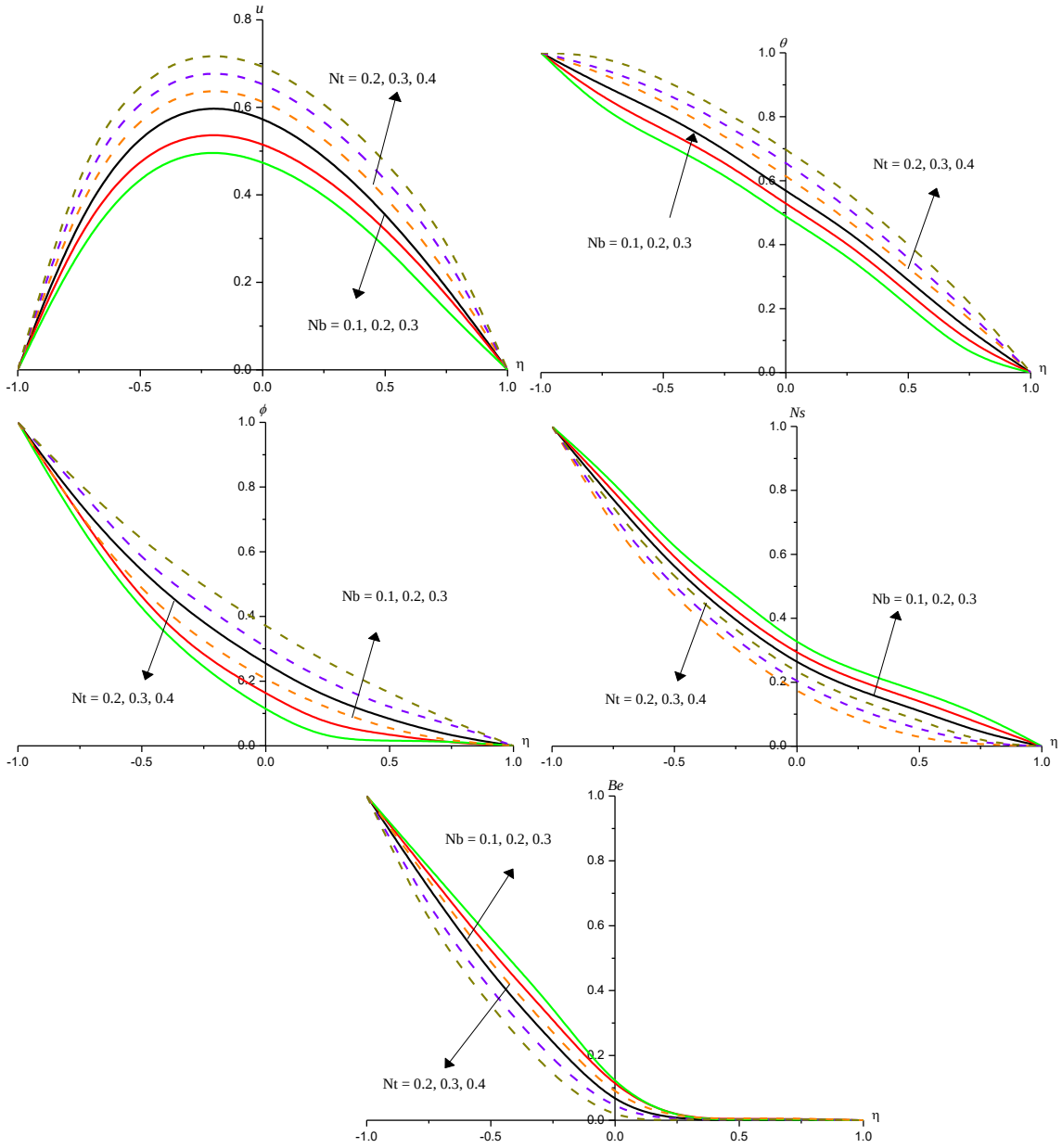

Fig.4 : Variation of [a]Velocity(u), [b] Temperature (θ), [c]Concentration (ϕ), Entropy generation(Ns) , [e] Bejan number (Be) with Nb & Nt
G=2, M=0.5, B=0.25, K=0.2, Rd=0.5, Ec=0.05, γ=±0.5, E1=0.1, δ=0.2, Sc=0.24,Q1=0.5, Br=0.25, λ=0.5

https://doi.org/10.5281/zenodo.14868720

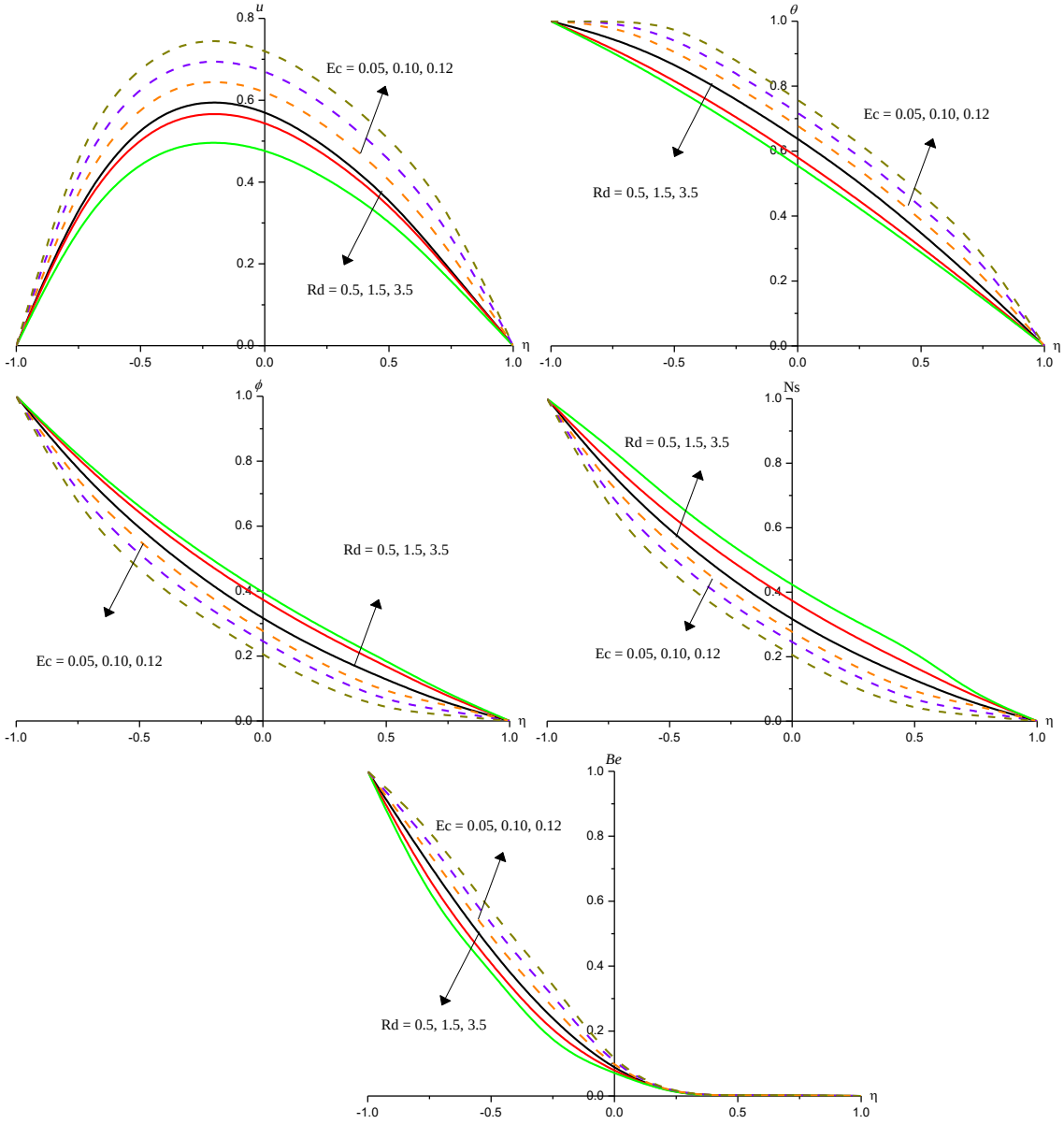

Fig.5 : Variation of [a]Velocity(u), [b] Temperature (θ), [c]Concentration (ϕ), Entropy generation(Ns) , [e] Bejan number (Be) with Rd & Ec
G=2, M=0.5, B=0.25, K=0.2, Nb=0.1, Nt=0.2, γ=±0.5, E1=0.1, δ=0.2, Sc=0.24,Q1=0.5, Br=0.25, λ=0.5

https://doi.org/10.5281/zenodo.14868720

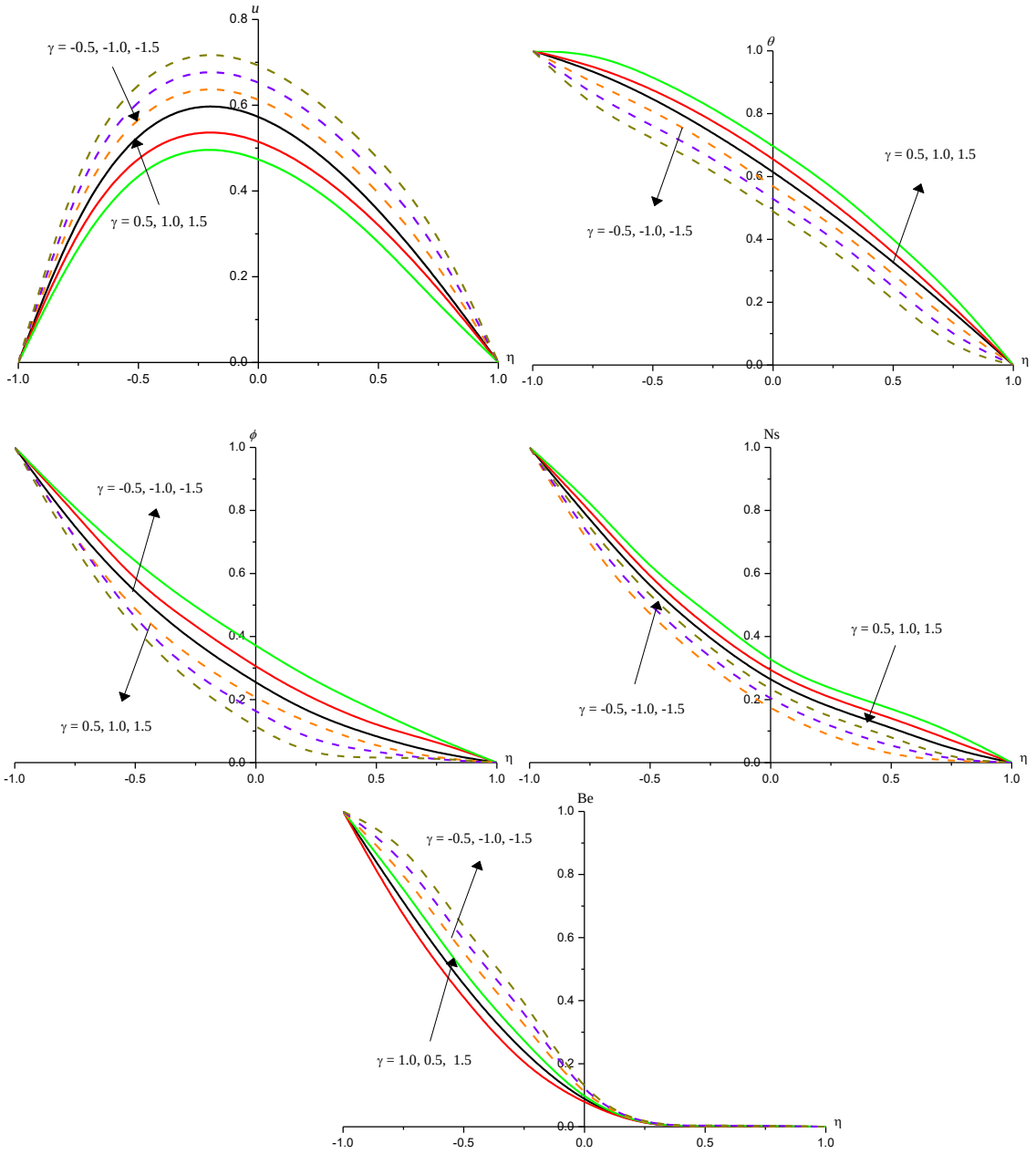

Fig.6 : Variation of [a] Velocity(u), [b] Temperature (θ), [c] Concentration (ϕ), Entropy generation(Ns) , [e] Bejan number (Be) with γ
G=2, M=0.5, B=0.25, K=0.2, Nb=0.1, Nt=0.2, Rd=0.5, Ec=0.05, E1=0.1, δ=0.2, Sc=0.24,Q1=0.5, Br=0.25, λ=0.5

https://doi.org/10.5281/zenodo.14868720

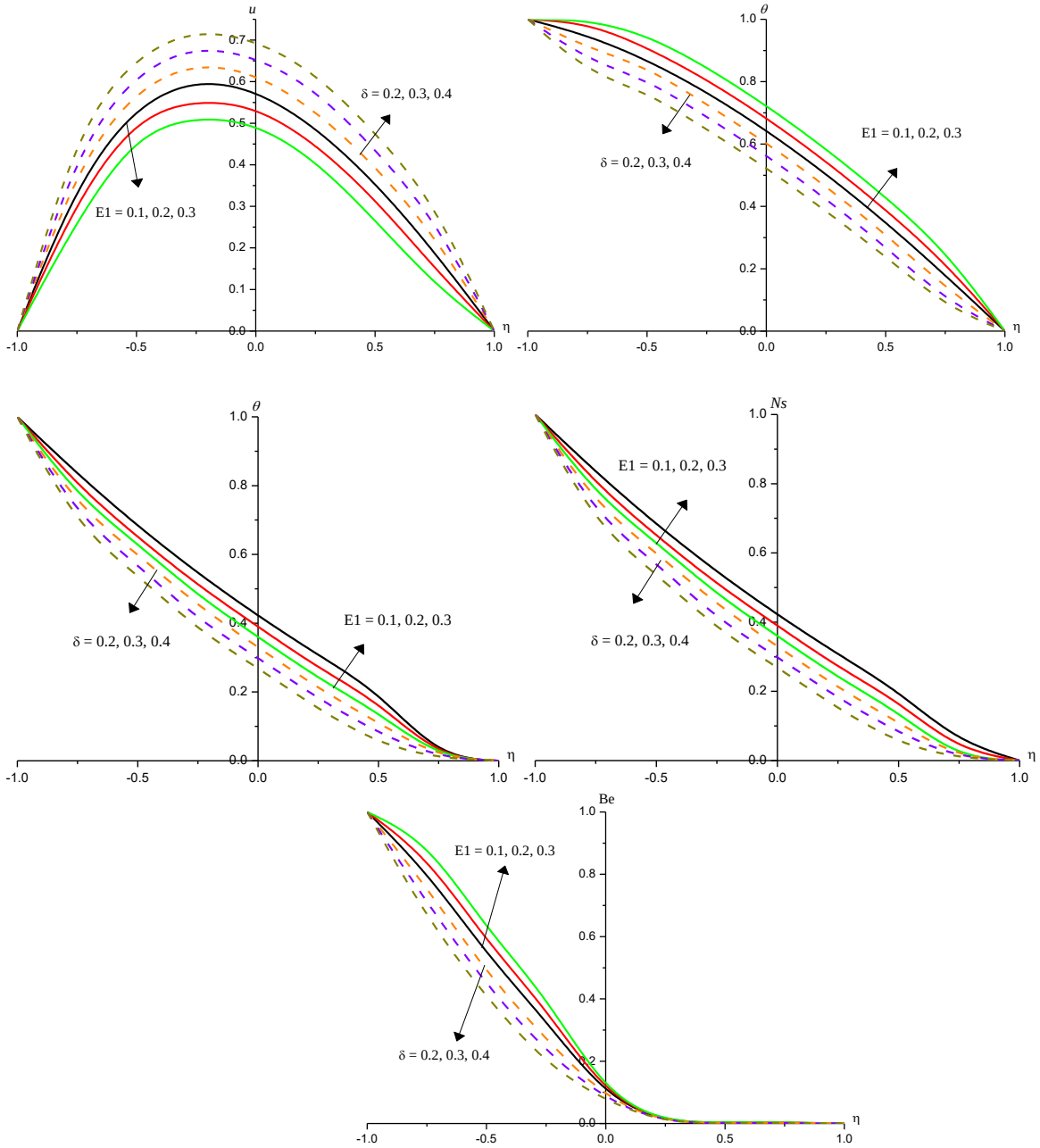

Fig.7 : Variation of [a] Velocity(u), [b] Temperature (θ), [c] Concentration (ϕ), Entropy generation(Ns) , [e] Bejan number (Be) with E1 & δ
G=2, M=0.5, B=0.25, K=0.2, Nb=0.1, Nt=0.2, Rd=0.5, Ec=0.05, γ=±0.5, Sc=0.24,Q1=0.5,Br=0.25, λ=0.5

https://doi.org/10.5281/zenodo.14868720

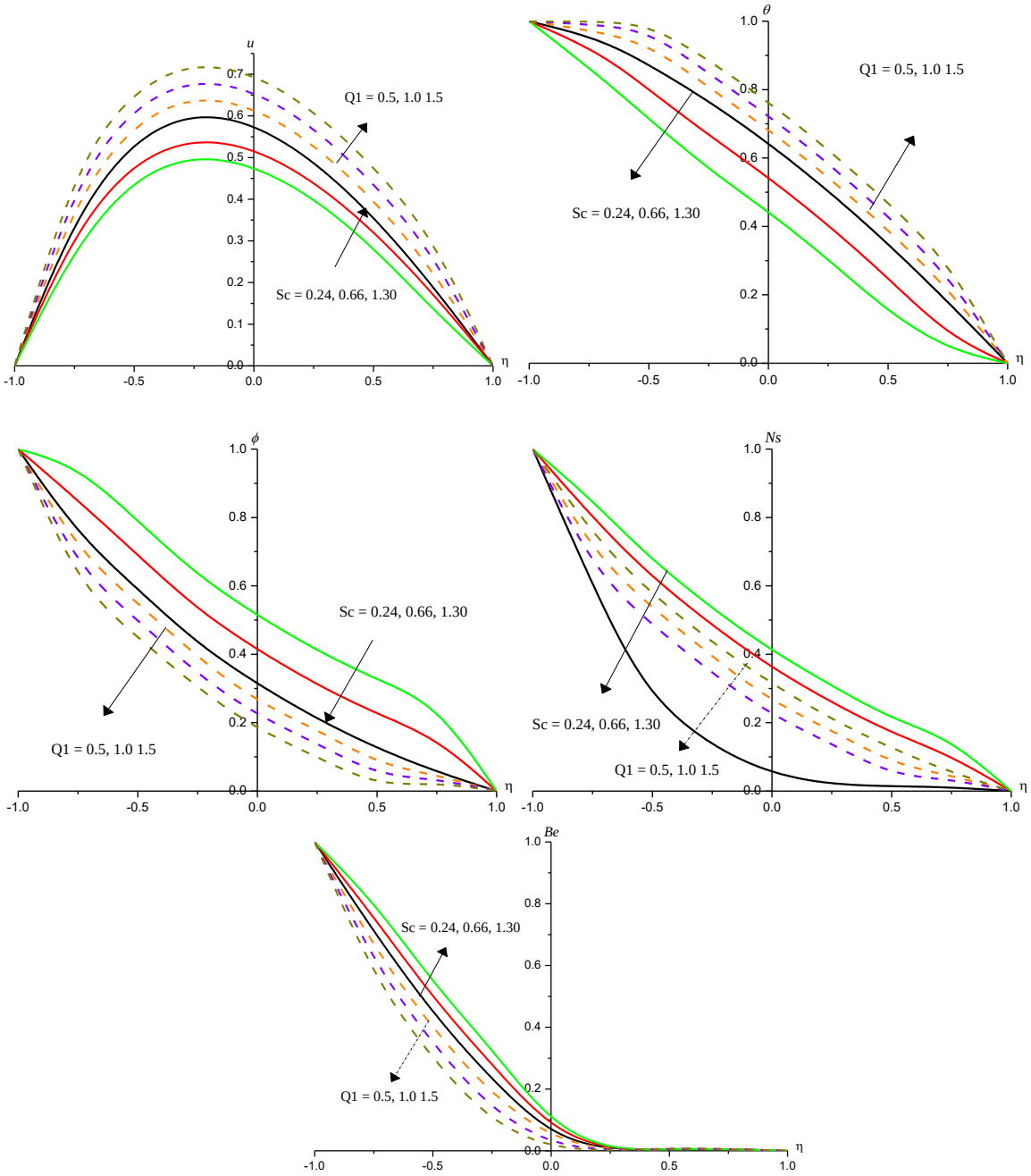

Fig.8 : Variation of [a]Velocity(u), [b]Temperature (θ), [c] Concentration (ϕ), Entropy generation(Ns) , [e] Bejan number (Be)with Q1 & Sc
G=2, M=0.5, B=0.25, K=0.2, Nb=0.1, Nt=0.2, Rd=0.5, Ec=0.05, γ=±0.5, E1=0.1, δ=0.2, Br=0.25, λ=0.5

https://doi.org/10.5281/zenodo.14868720

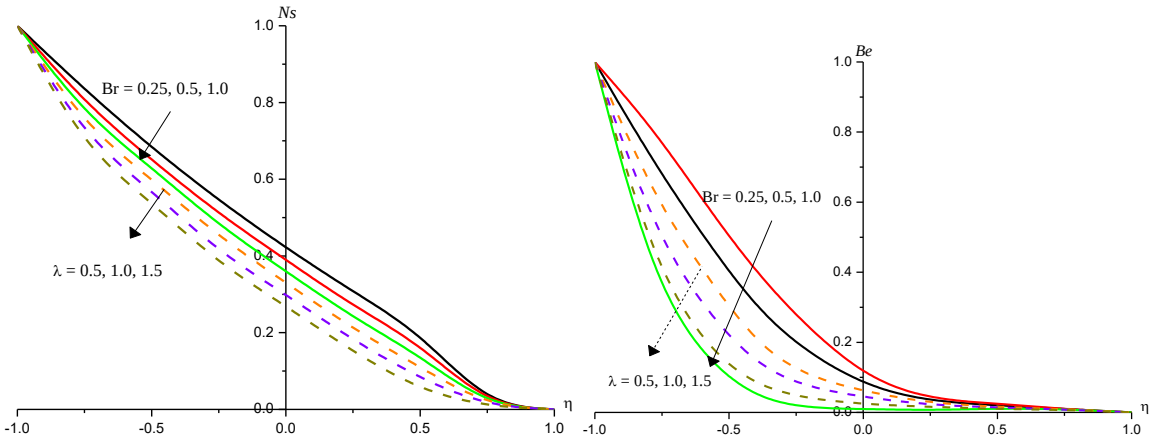

Fig.9 : Variation of [a] Entropy generation(Ns), [b] Bejan number (Be) with Br & λ

Table : 2: Skin friction (Cf), Nusselt(Nu) & Sherwood(Sh) numbers at η= ± 1

Parameter		Cf(-1)	Cf (+1)	Nu(-1)	Nu(+1)	Sh(-1)	Sh(+1)
G	2	1.85596	-0.805716	0.131711	0.748894	1.00059	0.200368
	4	2.03729	-0.853508	0.123646	0.754033	1.00836	0.195512
	6	2.22355	-0.902856	0.114568	0.759779	1.01711	0.190086
M	0.5	1.67955	-0.741367	0.136061	0.746515	0.99623	0.202747
	1.0	1.52778	-0.685324	0.139809	0.744317	0.99257	0.204917
	1.5	1.30913	-0.603252	0.145225	0.740863	0.98726	0.208255
K	0.2	1.85596	-0.805716	0.131711	0.748894	1.00059	0.200368
	0.4	1.75391	-0.763471	0.136754	0.745051	0.99575	0.204018
	0.6	1.68085	-0.733269	0.140143	0.742477	0.99841	0.206458
B	0.25	2.34266	-0.806058	0.125366	0.752117	1.00678	0.217383
	0.5	2.83838	-0.804424	0.119355	0.754767	1.01251	0.194929
	1.0	4.89383	-0.781247	0.098755	0.761399	1.03246	0.188899
Nr	0.2	1.85596	-0.805716	0.131711	0.748894	1.00059	0.200368
	0.4	1.75127	-0.790256	0.135293	0.747086	0.99718	0.202069
	0.6	1.52114	-0.716788	0.144572	0.740522	0.98819	0.208286
Rd	0.5	1.85596	-0.805716	0.131711	0.748894	1.00059	0.200368
	1.5	1.80256	-0.788651	0.288568	0.636479	0.85238	0.304708
	3.5	1.63034	-0.718367	0.354458	0.591994	0.78998	0.345967
Ec	0.05	1.85451	-0.805086	0.107426	0.766957	1.02396	0.183213
	0.10	1.85927	-0.806655	0.086708	0.782318	1.04399	0.168623
	0.12	1.86461	-0.808242	0.065709	0.797888	1.06411	0.153837
Nb	0.1	1.87016	-0.812764	0.176711	0.695008	1.35798	0.016236
	0.2	1.85605	-0.804904	0.110086	0.779161	0.90996	0.249798
	0.3	1.70362	-0.740945	0.090718	0.815508	0.83734	0.290449
Nt	0.2	1.86613	-0.810308	0.128318	0.761945	1.15488	0.083056
	0.3	1.87955	-0.815916	0.125843	0.771847	1.27515	-0.174378
	0.4	1.90668	-0.827498	0.127675	0.791112	1.51881	-0.227202
E1	0.1	1.85596	-0.805716	0.131711	0.748894	1.00059	0.200368
	0.2	1.85482	-0.805307	0.130561	0.750695	0.98035	0.206836

https://doi.org/10.5281/zenodo.14868720

ISSN: 0369-8963

Parameter		Cf(-1)	Cf (+1)	Nu(-1)	Nu(+1)	Sh(-1)	Sh(+1)
	0.3	1.69644	-0.739869	0.132496	0.756305	0.95678	0.217445
δ	0.2	1.84956	-0.803416	0.132526	0.747885	1.01289	0.197636
	0.3	1.85001	-0.803575	0.133045	0.747138	1.02326	0.195295
	0.4	1.85051	-0.803732	0.133558	0.746399	1.03356	0.192988
γ	0.5	1.85596	-0.805716	0.131711	0.748894	1.00059	0.200368
	1.0	1.85916	-0.806812	0.134874	0.744019	1.05906	0.183257
	1.5	1.90363	-0.809279	0.145453	0.733728	1.10693	0.173286
	-0.5	0.83964	-0.799889	0.122428	0.743646	0.83521	0.253629
	-1.0	1.83641	-0.798689	0.119076	0.768985	0.77989	0.273037
	-1.5	1.83785	-0.797725	0.116466	0.773275	0.73673	0.288721
S	0.3	1.85596	-0.805716	0.131711	0.748894	1.00059	0.200368
	0.5	2.01671	-0.721801	0.129936	0.745787	1.00241	0.203393
	0.7	1.98197	-0.604062	0.136578	0.738596	0.99613	0.210242
Sc	0.24	1.85596	-0.805716	0.131711	0.748894	1.00059	0.200368
	0.66	1.85916	-0.806812	0.134874	0.744019	1.05906	0.183257
	1.30	1.86317	-0.812128	0.144933	0.734518	1.09697	0.176008
Q1	0.5	1.86967	-0.809336	0.058868	0.780278	1.06994	0.171913
	1.0	1.88482	-0.813765	0.063240	0.802767	1.12291	0.151566
	1.5	1.90571	-0.819751	0.075883	0.832655	1.19849	0.124596
n	0.2	1.84819	-0.803003	0.131181	0.749826	0.98622	0.998767
	0.4	1.84837	-0.803059	0.131363	0.749563	0.98982	0.999876
	0.6	1.84855	-0.803115	0.131545	0.749356	0.99346	1.006576
Q	0.5	1.54335	1.553539	1.564736	1.527576	1.52016	1.514067
	1.0	0.72514	0.726631	0.072684	0.722681	0.72144	0.720384
	1.5	0.30267	0.204234	0.063245	0.462703	0.54288	0.611647
	-0.5	0.66528	0.779004	0.835328	0.568352	0.52348	0.486814
	-1.0	0.83846	0.930679	0.888275	0.686865	0.61086	0.545562
	-1.5	0.97673	0.988311	0.943525	0.365615	0.70681	0.6 40387
Pr	0.71	1.85232	-0.804357	0.116948	0.759887	1.01479	0.189929
	1.71	1.85631	-0.805674	0.099575	0.772774	1.03151	0.177688
	6.20	1.87697	-0.812261	0.082632	0.837204	1.11519	0.116515

8. CONCLUSION:

The effect of reaction rate parameter(Frank-Kameneskii constant)(Q1),variable viscosity (B)and activation energy (E1) on flow characteristics in a vertical channel is analysed. The findings of this analysis are:

i) An increase in viscosity parameter(B) enhances the velocity, temperature and reduces the nanoconcentratioin .The skin friction grows, Sherwood number enhances and Nusselt number decays at the left wall and opposite effect is seen in them at the right wall.

ii) Velocity enhances with increase in G/Ec/δ/Nt/γ>0/Sc and M/K/Nb/γ<0/E1.Increase in reaction rate parameter(Q1)results in growth of the momentum boundary layer thickness.

iii) Temperature enhances with G/Nb/Nt/Ec/γ>0/Sc and decays with M/K/Rd/γ<0/δ/Sc. Nanoconcentration enhances with M/K/Nb/Rd/γ<0/E1 and reduces with G/Nt/Ec/γ>0/δ.An

 https://doi.org/10.5281/zenodo.14868720

augmentation in reaction rate parameter(Q1) grows the thickness of the thermal boundary layer and decays the thickness of the solutal layer.

iv) Stress enhances with G/Nt/Ec/γ>0/Sc/Q1 and decays with M/K/Nb at $\eta=\pm1$.

v) Nu decay with G/Ec/E1/Q/Pr at η=-1 and enhances at η=+1.Nu enhances at η=-1 and reduces at η=+1. An opposite effect is seen in Nu at the walls with increase in M/K/Rd/γ/δ/Sc.

vi) Sherwood number(Sh)enhances at η=-1 and reduces at η+1 with increase in Ec/γ>0/δ/Sc/Q1. An opposite effect is seen in Sh with G/M/ K/Rd/E1/Pr.Sh grows at both walls with increase in Nt.

vii) Higher the activation energy results in an enhancement in entropy generation(Ns) and decay with larger values of temperature difference ratio(δ).the entropy generation(Ns) reduces with increase in both λ and $\mathrm{Br}\,\Omega^{-1}$.

viii) The Bejan number decreases with an increase in $\mathrm{Br}\,\Omega^{-1}$.

9. REFERENCES

[1]. Abbas S.Z., Ijaz Khan M., Kadry S., Khan W.A., Israr-UrRehman M., Waqas M., Fully developed entropy optimized second order velocity slip MHD nanofluid flow with activation energy, Comput. Methods Programs Biomed. (2020), https://doi.org/ 10.1016/j.cmpb.2020.105362.

[2]. Abbas S.Z., Khan W.A., Kadry S., Khan M.I., Waqas M., Khan M.I., Entropy optimized Darcy-Forchheimer nanofluid (Silicon dioxide, Molybdenum disulfide) subject to temperature dependent viscosity, Comput. Methods Programs Biomed. 190 (2020) 105363.

[3]. Adesanya S.O., Dairo O.F., Yusuf T.A., Onanaye A.S., Arekete S.A., Thermodynamics Analysis for heated gravity-driven hydromagnetic Couple Stress film with viscous dissipation effects, Physica A 540 (2020), https://doi.org/10.1016/ j.physa.2019.123150 123150.

[4]. Afridi M.I., Qasim M., Entropy Generation in ThreeDimensional Flow of Dissipative Fluid, Int. J. Appl. Comput. Math 4 (16) (2018) 1–11.

[5]. Buongiorno J., Convective transport in nanofluids, J. Heat Transf. 128 (2006) 240–250.

[6]. Das S., Chakraborty S., Jana R. N., Makinde O. D.. 2015. Entropy analysis of unsteady magneto-nanofluid flow past accelerating stretching sheet with convective boundary condition[J]. Appl. Math. Mech. -Engl. Ed., 36(12): 1593-1610.

[7]. Essma Belahmadi, Rachid Bessaih, Heat transfer and entropy generation analysis of Cu-water nanofluid in a vertical channel, World Journal of Engineering, 15(5): ISSN: 1708-5284, October 2018, DOI:10.1108/WJE-11-2017-0376

[8]. Gayathri, P : Impact of Variable Viscosity, Activation Energy on MHD Mixed Convective Heat and Mass Transfer Flow of a Nanofluid in a Cylindrical Annulus, *YMER :* Vol.21. Issue:4, PP:211-223, April-2022, ISSN : 0044-0477, www.ymerdigital.com

[9]. Gireesha B.J., M. Archana, B. Mahanthesh, Prasannakumara B.C., "Exploration of activationenergy and binary chemical reaction effects on nano Casson fluid flow with thermal and exponentialspace-based heat source", Multidiscipline Modeling in Materials and Structures, V.15 : 1, pp.227-245, (2019)

[10]. Hammed Abiodun Ogunseye ∗, Precious Sibanda, A mathematical model for entropy generation in a Powell-Eyring nanofluid flow in a porous channel, Heliyon 5 (2019) e01662, https://doi.org/10.1016/j.heliyon.2019.e01662

[11]. Ijaj Khan M, Sohail A, Khan, Hayat T, Imran Khan M and Alsaedi A : Arrchenius activation energy impact in binary chemically reactive flow of TiO_2-Cu-H2O hybird nanomaterial, International Journal of Chemical Reactor Engineering, (2018), DOI:10.1515/ijcre-2018-0183

[12]. Kahalerras H, Fersadou B, Nessab W, Mixed convection heat transfer and entropy generation analysis of copper–water nanofluid in a vertical channel with non‑uniform heating, SN Applied Sciences (2020) 2:76 | https://doi.org/10.1007/s42452-019-1869-2

[13]. Khan M.I., Qayyum S., Kadry S., Khan W.A., Abbas S.Z., Irreversibility Analysis and Heat Transport in Squeezing Nanoliquid Flow of Non–Newtonian (Second–Grade) Fluid between Infnite Plates with Activation Energy, Arabian J. Sci. Eng. 10.1007/s13369-020-04442-5.
[14]. Khan M.I.T, Hayat M, Khan I, and Alsaedi A: Activatio Energy impact in Nonlinear Radiative Stagnation Point Flow of Cross Nanofluid, Int.Communiations Heat Massachusetts Transfer, V.91, pp.216-224, (2018)
[15]. Michael Hamza Mkwizu, Oluwole Daniel Makinde : Entropy generation in a variable viscosity channel flow of nano fluids with convective cooling, *Comptes Rendus Mecanique*, 343 (2015) 38–56, http://dx.doi.org/10.1016/j.crme. 2014.09.002, www.sciencedirect.com
[16]. Mondal H., Almakki M., Sibanda P., Dual solutions for threedimensional magnetohydrodynamic nanofluid flow with entropy generation, J. Comput. Des. Eng. 6 (2019) 657–665.
[17]. Muhammad R., Ijaz Khan M., Magnetohydrodynamics (MHD) radiated nanomaterial viscous material flow by a curved surface with second order slip and entropy generation, Comput. Methods Programs Biomed. (2019), https://doi.org/10.1016/j. cmpb.2019.105294.
[18]. Nayak M.K., Abdul Hakeem A.K., Ganga B., Ijaz Khan M., Waqas M., Makinde O.D., Entropy optimized MHD 3D nanomaterial of non-Newtonian fluid: A combined approach to good absorber of solar energy and intensification of heat transport, Comput. Methods Programs Biomed. (2019), https:// doi.org/10.1016/j.cmpb.2019.105131.
[19]. Nidhish K. Mishra, Parikshit Sharma, Bhupendra K. Sharma, Bandar Almohsen, Laura M. P´erez: Electroosmotic MHD ternary hybrid Jeffery nanofluid flow through a ciliated vertical channel with gyrotactic microorganisms: Entropy generation optimization, Heliyon10 (2024) e25102, https://doi.org/10.1016/j.heliyon.2024.e25102
[20]. Rashidi M.M., Mohammadi F., Abbasbandy S., Alhuthali M.S., Entropy generation analysis for stagnation point flow in a porous medium over a permeable stretching surface, J. Appl. Fluid Mech. 8 (4) (2015) 753–765.
[21]. Reddy M.V., Lakshminarayana P., Cross-diffusion and heat source effects on a three-dimensional MHD flow of Maxwell nanofluid over a stretching surface with chemical reaction, Eur. Phys. J. Spec. Top. 230 (5) (2021) 1371–1379.
[22]. Riaz Muhammad M., Ijaz Khan, Mohammed Jameel, Niaz B. Khan, Fully developed Darcy-Forchheimer mixed convective flow over a curved surface with activation energy and entropy generation, Comput. Methods Programs Biomed. (2019), https://doi.org/10.1016/j.cmpb.2019.105298.
[23]. Saida Rashid, Tasawar Hayat, Sumaira Qayyum, Muhammad Ayub, Ahmed Alsaedi, "Threedimensionalrotating Darcy–Forchheimer flow with activation energy", Int. Journal of Numerical Methods for Heat & Fluid Flow, 29 : 3, pp.935-948, (2019)
[24]. Sandhya G, Sreelakshmi K, Sarojamma G, : Effect of Arrhenius activation energy and dual stratifications on the MHD flow of a Maxwell nanofluid with viscous heating, The International Journal of Engineering and Science (IJES), ISSN (e): 2319 – 1813 ISSN (p): 23-19 – 1805, pp.55-60, (2020)
[25]. Wang J., Muhammad R., Ijaz Khan M., Khan W.A., Abbas S.Z., Entropy optimized MHD nanomaterial flow subject to variable thicked surface, Comput. Methods Progr. Biomed. (2019), https://doi.org/10.1016/j.cmpb.2019.105311.
[26]. Woods L.C., Thermodynamics of Fluid Systems, Oxford University Press, Oxford, UK, 1975.
[27]. Yusuf T.A., Adesanya S.O., Gbadeyan J.A., Entropy generation in MHD Williamson nanofluid over a convectively heated stretching plate with chemical reaction, Heat Transfer. (2020) 1– 18, https://doi.org/10.1002/htj.21703.
[28]. Zaheer Abbas, Muhammad Naveed, Meriyem Hussain, Nadeem Salamat, Analysis of entropy generation for MHD flow of viscous fluid embedded in a vertical porous channel with thermal radiation, Alexandria Engineering Journal (2020) 59, 3395–3405, https://doi.org/10.1016/j.aej.2020.05.019
[29]. Zeeshan A., Shehzad N., Ellahi R., "Analysis of activation energy in Couette-Poiseuille flow of nanofluid in the presence of chemical reaction and convective boundary conditions", Results in Physics,V.8 ,pp. 502–512(2018).
[30]. Adeshina T. Adeosun, Joel C. Ukaegbu: Effect of the variable electrical conductivity on the thermal stability of the MHD reactive squeezed fluid flow through a channel by a spectral collocation approach, Partial Differential Equations in Applied Mathematics 5 (2022) 100256, https://doi.org/10.1016/j.padiff.2021.100256
[31]. Obalalu Adebowale Martins, Ajala Olusegun Adebayo, Adeshina Taofeeq Adeosun, Akintayo Oladimeji Akindele, Olayinka Akeem Oladapo, Olatunbosun Akintayo Olajide, Adegbite Peter : Significance of variable electrical conductivity on non-Newtonian fluid flow between two vertical plates in the coexistence of

Arrhenius energy and exothermic chemical reaction, Partial Differential Equations in Applied Mathematics 4 (2021) 100184, https://doi.org/10.1016/j.padiff.2021.100184

[32]. Obalalu AM, Ajala AO, Akindele AO, Oladapo OA, Adepoju O, Jimoh OM. Unsteady squeezed flow and heat transfer of dissipative casson fluid using optimal homotopy analysis method: An application of solar radiation. *Partial Diff Equ Appl Math*. 2021:100146. http://dx.doi.org/10.1016/j.padiff.2021.100146.

[33]. Obalalu AM, Ajala OA, Abdulraheem A, Oladimeji AA. The influence of variable electrical conductivity on non-Darcian Casson nanofluid flow with first and second-order slip conditions. *Partial Diff Equ Appl Math*. 2021:100084. http://dx.doi.org/10.1016/j.padiff.2021.100084.

[34]. Balakrishnan E, Swift A, Wake GC (1996). Critical values for some non-class A geometries in thermal ignition theory. Math. Comput. Modell., 24: 1–10.

[35]. Bowes PC (1984). Self-heating: Evaluating and controlling the hazard. Amsterdam: Elsevier Sciences.

[36]. Lohrer C, Schmidt M, Krause U (2005). A study on the influence of liquid water and water vapour on the self-ignition of lignite coal – experiments and numerical simulations. J. Loss Prevent Proc. Ind., 18(3): 167–177.

[37]. Makinde OD (2004). Exothermic explosions in a slab: A case study of series summation technique. Int. Comm. Heat Mass Trans., 31(8): 1227-1231.

[38]. Simmie JM (2003). Detailed chemical kinetic models for the combustion of hydrocarbon fuels. Prog. Energy Combust. Sci., 29: 599–634.

[39]. Tanaka S, Ayala F, Keck JC (2003). A reduced chemical kinetic model for HCCI combustion of primary reference fuels in a rapid compression machine. Combust. Flame, 133: 467–481.

[40]. Williams FA (1985). Combustion theory. Second Edition, Benjamin & Cuminy publishing Inc. Menlo Park, Califonia.

[41]. Legodi and Makinde : A numerical study of steady state exothermic reaction in a slab with convective boundary conditions, International Journal of the Physical Sciences Vol. 6(10), pp. 2541-2549, 18 May, 2011, http://www.academicjournals.org/IJPS, DOI: 10.5897/AJBM11.307.

[42]. Nagasasikala M : Effect of activation energy on convective heat and mass transfer flow of dissipative nanofluid in vertical channel with brownian motion and thermophoresis in the presence of irregular heat sources, World Journal of Engineering Research and Technology (WJERT), www.wjert.org, *2023, Vol. 9, Issue 2, XX-XX,* ISSN 2454-695X